

# Vibro-acoustical Behavior of a Turbocharger Housing Excited by Oil-film Induced Rotor Oscillations

A. Boyaci, W. Seemann

*This paper deals with the interaction of the turbocharger housing and the rotor to reveal the acoustic phenomena which are excited by the oil whirl/whip instabilities. Therefore, a flexible multibody model is built up for the rotor subsystem which is supported in floating ring bearings. The flexibility of the housing subsystem is taken into account by considering it as a modally reduced structure within the multibody simulation model. Primarily, the two subsystems are simulated sequentially. The first step gives the oil film forces during a typical run-up simulation of the rotor subsystem if the bearing shell deformation is neglected. In a second step, the obtained oil film forces are applied at the decoupled housing structure to analyze the vibro-acoustics of the turbocharger in detail. The vibro-acoustical behavior is judged by the occurring housing amplitudes which are predominantly influenced by the mounting concept of the turbocharger on the engine. It is found out that the subsynchronous excitation due to the oil films can be magnified through the housing structure in a quite wide speed range which is the main excitation mechanism affecting the acoustics of turbochargers. Finally, the run-up simulation is performed for the coupled subsystems of rotor and housing where the oil film forces are also dependent on the local deformation of the bearing housing.*

## 1 Introduction

High-speed rotors in turbochargers are well-known to show synchronous oscillations due to unbalance as well as various types of subsynchronous oscillations which are induced by several whirl/whip instabilities of the oil films. The rotor oscillations are transmitted through the nonlinear oil film forces to the turbocharger housing whose acoustic emission significantly affects the driver comfort especially in passenger-car applications.

Floating ring bearings are usually chosen to support the turbocharger rotors where the inner and the outer oil films causes different types of subsynchronous oscillations (Orcutt and Ng, 1968; Tanaka and Hori, 1972) which are basically in the conical and cylindrical forward rotor mode, respectively. With regard to the oil film generating the subsynchronous frequency and the rotor mode shape, Schweizer (2009, 2010) suggested a categorization of the occurring types of subsynchronous oscillations (Sub 1: conical mode, inner oil film; Sub 2: cylindrical mode, inner oil film; Sub 3: conical mode, outer oil film) which is also adopted in this study, see also (Boyaci and Schweizer, 2015). Furthermore, typical bifurcation sequences are shown by performing transient run-up simulations of the rotor bearing systems. Recently, run-up simulations are carried out by applying more sophisticated bearing models (Chasalevris, 2016) where, for instance, the bearing geometry with feeding holes and grooves is taken into account (Nowald et al., 2015; Woschke et al., 2015). The influence of design parameters on the subsynchronous oscillations is systematically investigated in (Koutsovasilis et al., 2015). The methods of numerical continuation can be applied to investigate the stability behavior of floating ring bearings in detail (Boyaci et al., 2009, 2011, 2015; Boyaci, 2016) and to detect the types of bifurcations at the critical speeds. The additional consideration of the thrust bearing leads to the damping of the subsynchronous oscillations where the conical rotor modes are involved (Chatzisavvas et al., 2016). Transient simulations are also validated with experimental measurements in (Kirk et al., 2007; Köhl et al., 2014; San Andrés et al., 2007).

The failure of floating ring bearings probably causes a rotor damage which is known as Total Instability (Schweizer, 2009) represented by the critical limit cycle (Boyaci et al., 2011). In this case, the flexibility of the bearing housing can become essential on the occurrence of the subsynchronous oscillations and is therefore simply modeled as linear spring-damper element in (Schweizer, 2009). Moreover, oil-film-induced acoustic problems of turbochargers are reported in many publications, e.g. (Nguyen-Schäfer, 2013), but not explicitly analyzed by modeling both the rotor and the housing structure. In order to improve the vibro-acoustical behavior, the physical understanding

of the interaction between rotor and housing, especially the mechanism of transmitting the oil film forces, is an important part of the research in subsynchronous oscillations of turbochargers.

Within this paper, the next section outlines the flexible multibody model of the investigated turbocharger rotor/housing system. The modal analysis of the housing structure gives hints which modes can become significant for the vibro-acoustical behavior. In Section 3, the constant-tone phenomenon is first explained by a sequential simulation of the decoupled subsystems rotor and housing where a typical bifurcation sequence of subsynchronous oscillations is considered. Then, the effect of the bearing shell deformation is examined on the subsynchronous oscillations for the coupled subsystems. Finally, the decoupled and the coupled approach are compared with each other. Section 4 shortly summarizes the paper.

## 2 Mechanical Model

### 2.1 Flexible Multibody Model of Turbocharger Rotor/Housing System

The interaction of the turbocharger rotor and housing is investigated by a flexible multibody model. The turbocharger rotor/housing system can be disassembled into two subsystems whose interfaces are the two radial bearings. As depicted in Figure 1 (a), the multibody model of the turbocharger rotor consists of a flexible shaft

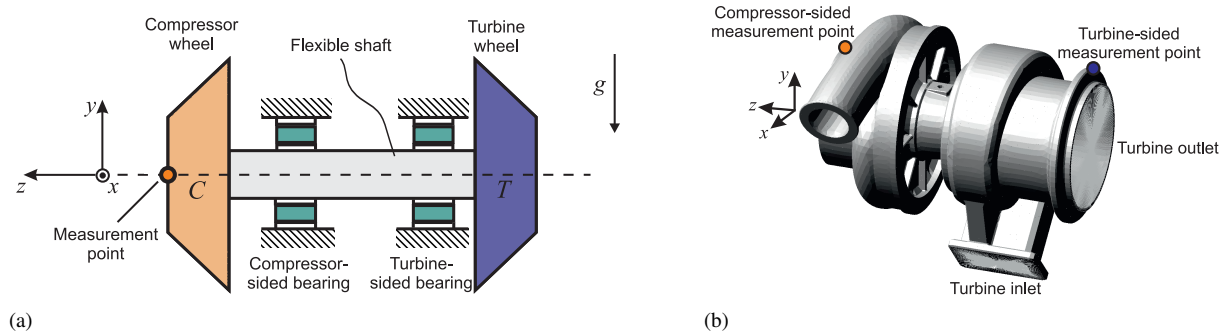


Figure 1: Mechanical model of subsystems: (a) Turbocharger rotor. (b) Housing structure.

at which two rigid disks are placed representing the compressor and the turbine wheel. The flexible shaft is incorporated as a modally reduced structure by applying component mode synthesis which is described in (Craig and Bampton, 1968; Shabana, 2005). The rotor is supported by two full-floating ring bearings where the rings are assumed to be rigid bodies with two translational and one rotational degree of freedom. The nonlinear oil film forces are given by analytical expressions, see e.g. (Boyaci et al., 2015; Childs, 1993), which can be derived by the short bearing theory of DuBois and Ocvirk (1953). Unbalance is modeled by two point masses which are attached on the compressor and turbine wheel. The complete housing structure is also discretized by finite elements and modally reduced by component mode synthesis. The system is under the influence of earth's gravitational field  $g$ . Axial and torsional motions of the multibody system are neglected in this study.

Analogously as for instance in (Chatzisavvas et al., 2016; Koutsovasilis et al., 2015; Schweizer, 2009, 2010), the flexible multibody model of the turbocharger rotor/housing can be stated as a system of nonlinear Differential-Algebraic Equations (DAEs) which is here written in the stabilized index-2 formulation (Ascher and Petzold, 1998)

$$\begin{aligned} \mathbf{M}(\mathbf{q}) \dot{\mathbf{u}} &= \mathbf{f}(\mathbf{q}, \mathbf{u}, t) - \mathbf{G}^T(\mathbf{q}, t) \boldsymbol{\lambda}, & \dot{\mathbf{q}} &= \mathbf{u} - \mathbf{G}^T(\mathbf{q}, t) \boldsymbol{\mu}, \\ \mathbf{0} &= \mathbf{g}(\mathbf{q}, t), & \mathbf{0} &= \mathbf{G}^T(\mathbf{q}, t) \mathbf{u} + \frac{\partial \mathbf{g}}{\partial t}(\mathbf{q}, t), \end{aligned}$$

and which is computed by using solvers based on the backward differentiation formula (Gear et al., 1985). The vectors  $\mathbf{q}$  and  $\mathbf{u}$  collect the generalized coordinates and velocities, respectively, which also include the modal coordinates of the flexible bodies. The symmetric positive definite mass matrix is given by  $\mathbf{M}(\mathbf{q})$ . The vector  $\mathbf{f}(\mathbf{q}, \mathbf{u}, t)$  represents all applied and gyroscopic forces. The algebraic constraint equations are considered in  $\mathbf{g}(\mathbf{q}, t)$  from which the Jacobian  $\mathbf{G}(\mathbf{q}, t) = \frac{\partial \mathbf{g}}{\partial \mathbf{q}}$  is obtained. Then,  $-\mathbf{G}^T(\mathbf{q}, t) \boldsymbol{\lambda}$  describes the constraint forces where  $\boldsymbol{\lambda}$  is the vector of Lagrange multipliers. To avoid the drift-off effect when solving the DAE, the correction term  $-\mathbf{G}^T(\mathbf{q}, t) \boldsymbol{\mu}$  is added to the equations by introducing auxiliary Lagrange multipliers  $\boldsymbol{\mu}$ .

## 2.2 Modal Analysis of Turbocharger Housing Subsystem

Before the transient simulations are presented, the modal behavior of the turbocharger housing ( $m_H \approx 5$  kg) is discussed to support the result interpretation of the subsequent simulations. As shown in Figure 1, the housing structure is built up of two assembled sections which are the compressor-side section and the turbine-side section including the bearing housing. Furthermore, to model the mounting of the turbocharger on the engine block, it is assumed that the housing is rigidly clamped at both the turbine inlet (twin scroll) and outlet while free boundary conditions are chosen at the compressor side. Then, the modal analysis yields the eigenfrequencies and corresponding mode shapes of the housing (cf. Figure 2). Note that the modal behavior of the housing is strongly dependent on the chosen boundary conditions.

Figure 2 outlines four modes of the clamped housing structure which are excited by the oil film forces in the next section. The axial and torsional modes as well as the higher modes of the turbocharger housing are not explicitly considered here since they can hardly be observed directly in the transient simulations. Primarily, it

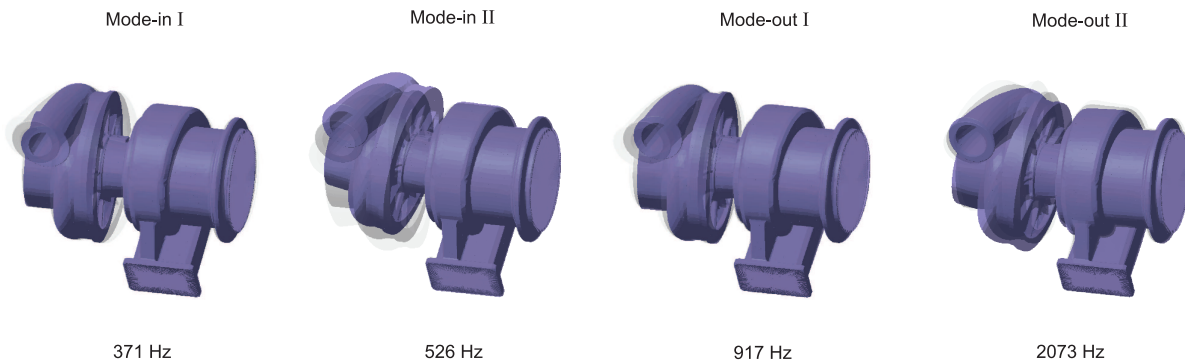


Figure 2: Modal analysis of housing structure which is rigidly clamped at the turbine inlet and outlet.

can be distinguished between two types of bending modes by considering the phase difference of the compressor and turbine section. In-phase oscillations of both sections characterize the first in-phase bending modes – Mode-in I and Mode-in II – about the principal axes of the housing. The two further bending modes – Mode-out I and Mode-out II – describe out-of-phase oscillations of both sections where the nodal point is located close to the turbine-sided bearing. However, for all types of modes, the amplitudes at the turbine section are much lower since the fixed clamping is applied on this side.

## 3 Run-up Simulation

In this section, a small-sized (passenger-car) turbocharger is considered to investigate the rotor-housing interaction. The multibody simulation model comprises two different subsystems which are, on the one hand, the nonlinear rotor subsystem (rotor mass  $m_R \approx 0.2$  kg, rotor length  $\ell_R \approx 130$  mm) supported in full-floating ring bearings and, on the other hand, the linear housing subsystem (housing mass  $m_H \approx 5$  kg). The coupling between the two subsystems is modeled in two different ways. The first approach is to simulate both subsystems sequentially and thus separately. For this purpose, a run-up simulation of the rotor subsystem is primarily performed to obtain the nonlinear oil film forces where the bearing shell as part of the housing structure is assumed to be rigid. In a further transient simulation, the nonlinear oil film forces are applied as external excitations on the bearing shells to compute the housing oscillations. With regard to the decoupled subsystems, the rotor subsystem only affects the housing oscillations but not vice versa. Therefore, in the second approach, both subsystems are fully coupled and a transient run-up simulation is performed for the complete system. Consequently, the elastic deformation of the bearing shells is also considered on the rotor oscillations so that both subsystems mutually interact with each other.

### 3.1 Decoupled Subsystems

#### 3.1.1 Rotor Bearing Subsystem

Figure 3 shows the run-up simulation of the decoupled rotor subsystem where the rotor speed is prescribed by an increasing linear time function from rest up to 3500 Hz. As already depicted in Fig 1 (a), the nonlinear oscillations are evaluated by studying the vertical displacement of the compressor-sided measurement point and the relative bearing eccentricities (compressor-sided inner/outer and turbine-sided inner/outer oil films). Additionally, the waterfall diagram in two aspects illustrates the synchronous and subsynchronous frequencies as well as the amplitudes of the compressor-sided displacement. Here, the run-up simulation reveals the following characteristic bifurcation sequence (cf. Figure 3) which comprises the three types of subsynchronous oscillations Sub 1 → Sub 2 → Sub 2/3 (MM):

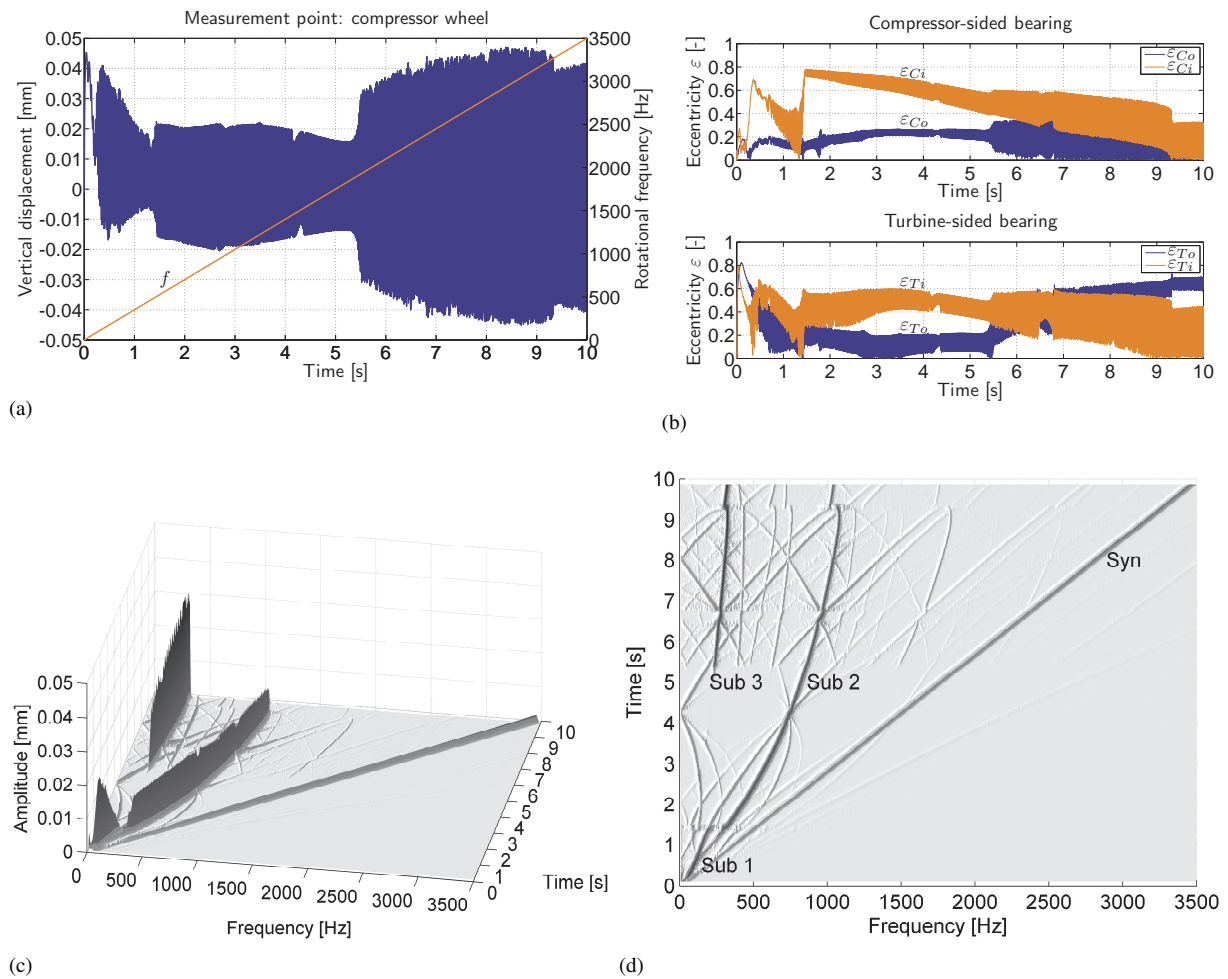


Figure 3: Run-up simulation of decoupled rotor bearing subsystem: (a) Vertical displacement of measurement point at compressor side (blue), rotational frequency  $f$  (red). (b) Compressor-sided inner/outer and turbine-sided inner/outer bearing eccentricities. (c)-(d) Waterfall diagrams (3D- and top-view) of plot (a).

- By increasing the rotational frequency from rest, the rotor bearing system needs a certain settling time before the Sub 1 oscillations are fully observed at  $f \approx 105$  Hz ( $t \approx 0.3$  s). They show the typical high inner bearing eccentricities of both bearings as well as the subsynchronous frequency which is associated with the conical forward rotor mode.
- Upon passing through the Sub 1 oscillations, they become unstable at  $f \approx 490$  Hz ( $t \approx 1.4$  s) and directly bifurcate to the Sub 2 oscillations which are characterized by a cylindrical forward rotor mode. In addition to the high inner bearing eccentricities, the subsynchronous frequency points to the inner oil films as source of the whirl/whip instability.

- In contrast to Sub 1, the Sub 2 oscillations remain apparent in the whole operation speed range up to 3500 Hz. However at  $f \approx 1890$  Hz ( $t \approx 5.4$  s), a further bifurcation leads to a Sub 3 component with a relatively much lower subsynchronous frequency which corresponds to a whirl/whip instability due to the outer oil films. In the case of Sub 3, the rotor mode shape is a conical forward one. By increasing the rotor speed from  $f \approx 1890$  Hz ( $t \approx 5.4$  s), the resulting rotor oscillations describe mixed-mode solutions of Sub 2 and Sub 3 which are denoted by Sub 2/3 (MM). The Sub 3 amplitudes grow with higher rotor speeds while the Sub 2 amplitudes remain nearly constant. Due to the higher Sub 3 amplitudes, the Sub 3 component prevails over Sub 2 during the occurrence of the mixed-mode oscillations.

To recapitulate briefly, this run-up simulation represents a classical bifurcation scenario of a small-sized turbocharger rotor bearing system. Since all three types of subsynchronous oscillations occur, it is convenient to use this reference simulation for demonstrating the vibro-acoustical behavior of the turbocharger housing.

### 3.1.2 Turbocharger Housing Subsystem

As noted above, the flexibility of both bearing shells is not taken into account to calculate the rotor oscillations as well as the nonlinear oil film forces. Therefore, the previously computed oil film forces lead to the excitation of the decoupled linear housing subsystem by the synchronous and the various subsynchronous frequencies in the spatial  $x$ - and  $y$ -direction, respectively. Then, the response amplitudes are significantly dependent on the modal properties of the housing structure. Figure 4 depicts the simulation results which represent the normalized housing displacements in  $x$ - and  $y$ -direction of both bearing shells, cf. Figure 1 (b). Hereafter, the housing displacements are always normalized with respect to the outer bearing clearance  $C_o$ . The response frequencies and amplitudes can be representatively taken from the waterfall diagram of the housing displacement in  $x$ -direction.

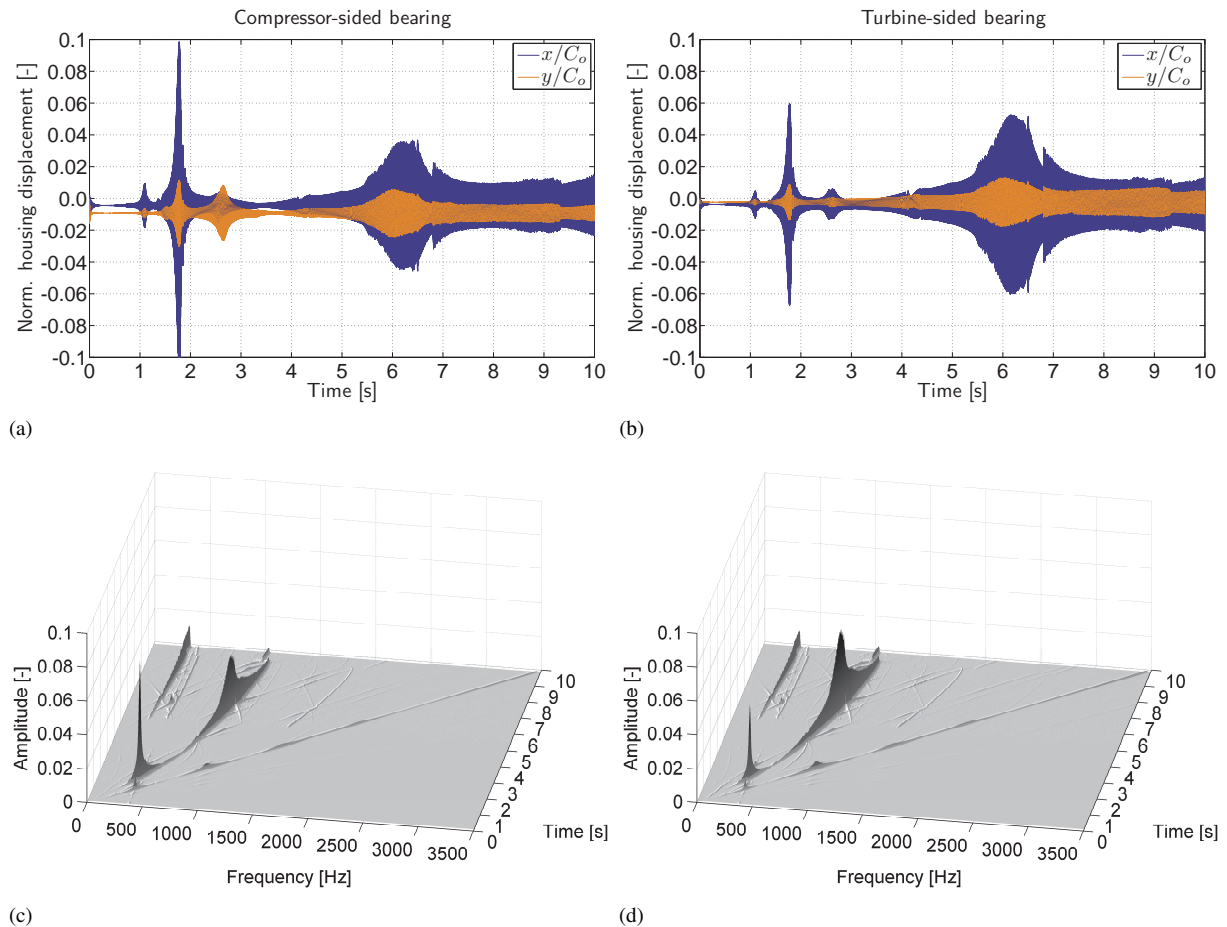


Figure 4: Transient simulation of decoupled housing subsystem: (a) Normalized housing displacement at compressor-sided bearing. (b) Normalized housing displacement at turbine-sided bearing. (c) Waterfall diagram of displacement in  $x$ -direction from plot (a). (d) Waterfall diagram of displacement in  $x$ -direction from plot (b).

If the synchronous frequency due to unbalance and the subsynchronous frequencies due to the oil films equal one of the eigenfrequencies, resonances of the housing structure can be observed in the operation speed range where four resonance peaks are clearly pronounced:

- The synchronous component of the oil film forces excites the first housing mode Mode-in I at  $t \approx 1.1$  s ( $f \approx 385$  Hz) where the compressor- and turbine-sided housing part apparently undergo in-phase oscillations.
- The second resonance peak again corresponds to Mode-in I at  $t \approx 1.8$  s ( $f \approx 630$  Hz). However, the excitation comes from the Sub 2 component of the oil film forces. Due to the higher amplitudes of the Sub 2 oscillations for the decoupled rotor subsystem (cf. Figure 3), the housing amplitudes are accordingly larger than in the case of the first resonance peak.
- The synchronous excitation leads to the resonance of Mode-out I at  $t \approx 2.6$  s ( $f \approx 910$  Hz) which describes out-of-phase oscillations of the compressor- and turbine-sided housing part.
- The Sub 2 excitation also gives a resonance of Mode-out I at  $t \approx 6.2$  s ( $f \approx 2170$  Hz) which reveals higher amplitudes than for the synchronous excitation. However, the amplitudes are still lower than for the Sub 2 excitation of the in-phase mode (Mode-in I). Since the Sub 2 frequency nearly remains constant in that speed range the resonance is slower-passed through. Thus, the resonance region becomes much broader so that a magnification of the Sub 2 is obtained for a wider speed range. The Sub 2 excitation with an almost constant frequency is also widely known as the constant-tone phenomenon (Nguyen-Schäfer, 2013).

Furthermore, it has to be remarked that the elastic deformation of the bearing shells is up to maximal 10% of the outer clearance  $C_o$  when the Sub 2 excitation reaches the first housing eigenfrequency  $f_{eig} = 371$  Hz of Mode-in I. For Mode-out I at an eigenfrequency of  $f_{eig} = 917$  Hz, the shell deformation attains values up to 5% of  $C_o$  while it does not exceed approximately 1% in speed ranges away from resonances. Therefore, the influence of the shell deformation is small on the rotor oscillations as shown in the next subsection. A further observation is that Mode-in II at an eigenfrequency of  $f_{eig} = 526$  Hz is not obviously excited where a clear resonance peak occurs. A frequency response analysis reveals that the node of Mode-in II is located very close to the bearing locations and thus the point of application of both excitation forces. For this reason, Mode-in II plays only a negligible role in the resulting housing oscillations. Moreover, it seems that the subsynchronous frequencies of Sub 3 are too low to excite an eigenfrequency of the housing structure which means that the Sub 2 excitation is only magnified and finally may cause acoustic problems. Note that the synchronous excitation can become critical as well for higher unbalances.

For the sake of completeness, Figure 5 outlines the housing displacements in each of the three spatial directions  $x$ ,  $y$ ,  $z$  at the compressor- and turbine-sided measurement point. As before, the four resonance peaks are visible. The corresponding waterfall diagrams are omitted to illustrate in Figure 5 which bring no additional knowledge. The amplitudes of the compressor-sided measurement point are generally higher since the housing is rigidly supported on the turbine side.

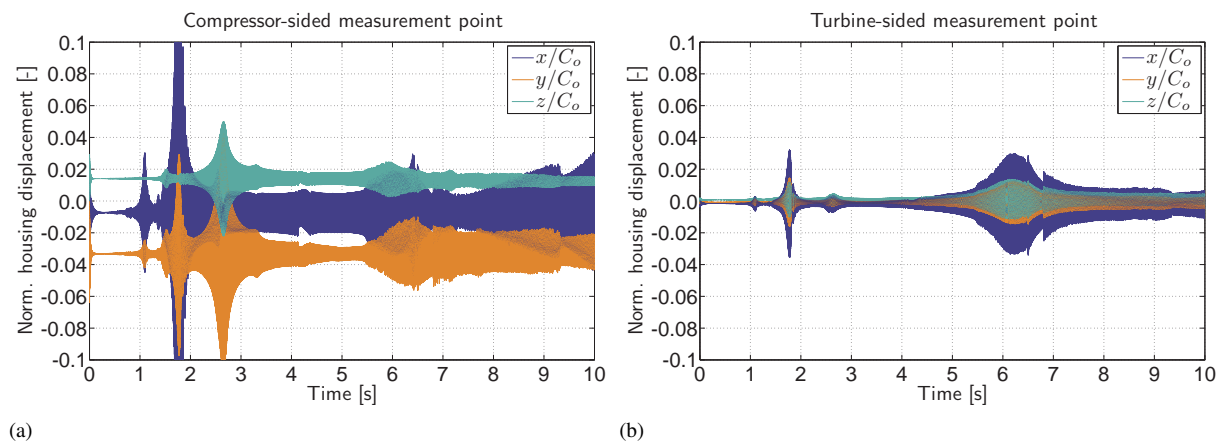


Figure 5: Normalized housing displacements for transient simulation of housing subsystem: (a) Compressor-sided measurement point. (b) Turbine-sided measurement point.

Thus, the vibro-acoustical behavior is significantly dependent on both the oil-film-induced excitation and the modal behavior of the turbocharger housing. Furthermore, the stability and bifurcation behavior of the rotor bearing system is difficult to judge if experimental measurements are only performed at points on the housing.

### 3.2 Coupled Subsystems

#### 3.2.1 Rotor Bearing Subsystem

According to the previous investigations, the run-up simulation is carried out here for the coupled subsystems of rotor and housing. Figure 6 illustrates the results of the rotor subsystem which are compared to the decoupled case from Figure 3:

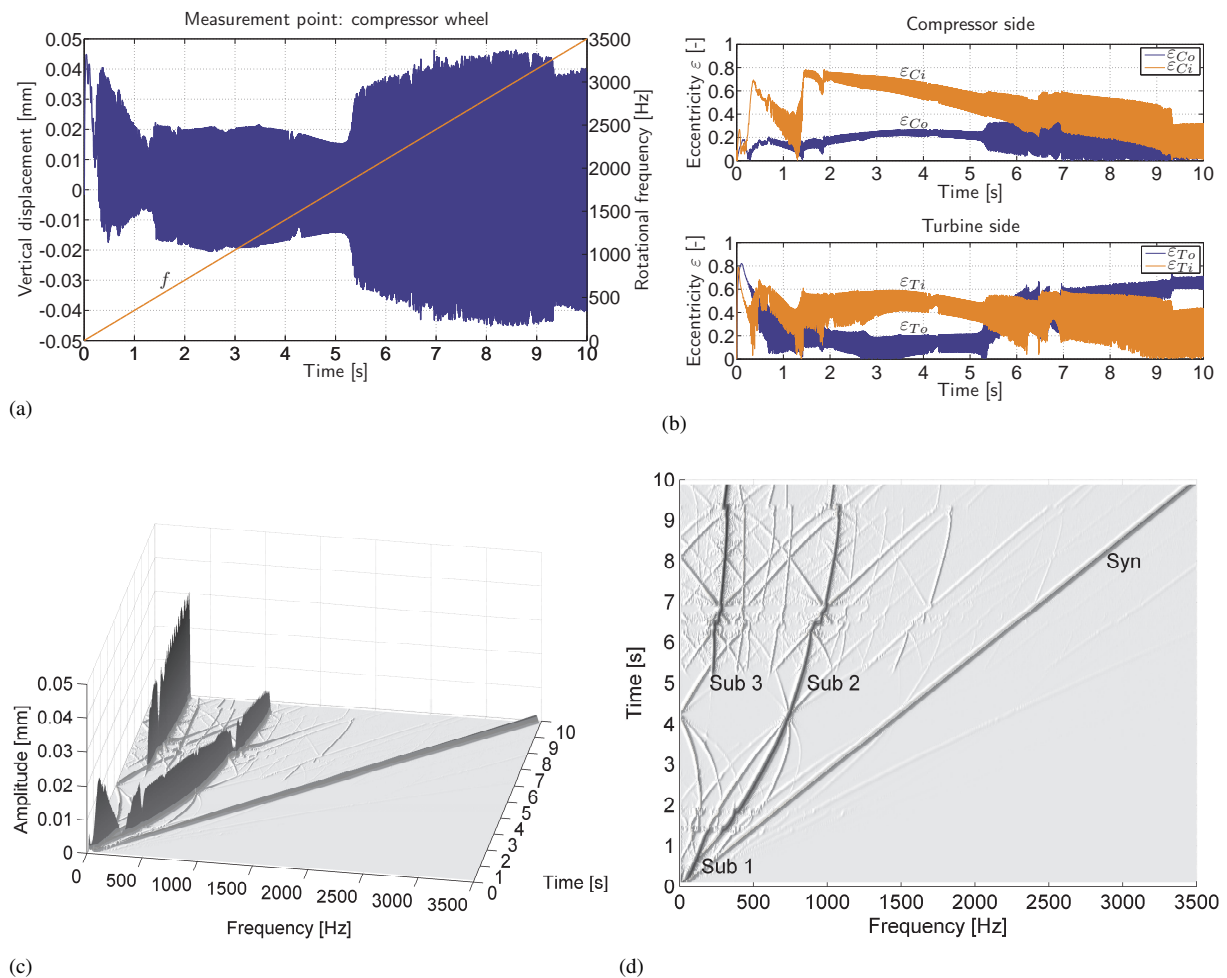


Figure 6: Run-up simulation of complete system (rotor subsystem): (a) Vertical displacement of measurement point at compressor side (blue), rotational frequency  $f$  (red). (b) Compressor-sided inner/outer and turbine-sided inner/outer bearing eccentricities. (c)-(d) Waterfall diagrams (3D- and top-view) of plot (a).

- The amplitudes of the rotor oscillations as well as the bearing eccentricities remain basically unaffected in the operation speed range.
- The subsynchronous frequencies are slightly diminished due to the additional flexibility through the bearing shells.
- Hence, the critical speeds are marginally reduced at which the types of subsynchronous oscillations occur and abruptly change, respectively.

- The main resonances of the housing structure, which are excited by Sub 2, can be traced back especially to the inner bearing eccentricity of the compressor-sided bearing and the subsynchronous frequencies. They both suddenly alter in the region of the resonance peaks and recover again very quickly after passing through.

As before supposed, the dynamical behavior of the rotor bearing system can be computed with a very good approximation by assuming rigid bearing shells. Note that the effect of shell deformation may become important on rotor oscillations in speed ranges where resonances of the housing structure occur. However, it is also conceivable that, with regard to Total Instability (Schweizer, 2009), high eccentricities associated with extremely high oil film forces can yield a bearing shell deformation which influences the rotor oscillations.

### 3.2.2 Turbocharger Housing Subsystem

Figure 7 shows the housing displacements and their oscillation frequencies at the bearing locations of the coupled housing subsystem. Compared to Figure 4, the following differences can be recognized:

- The oscillation amplitudes of the housing displacements are generally slightly lower than for the decoupled subsystems. This amplitude decrease is more pronounced for Mode-out I ( $f_{eig} = 917$  Hz).
- Due to the lower subsynchronous frequencies, the Sub 2 excitation leads to housing resonances which are shifted to higher rotor speeds. The resonance peak of the Mode-in I appears at  $t \approx 1.85$  s ( $f \approx 648$  Hz) while the one of Mode-out I at  $t \approx 6.5$  s ( $f \approx 2275$  Hz).

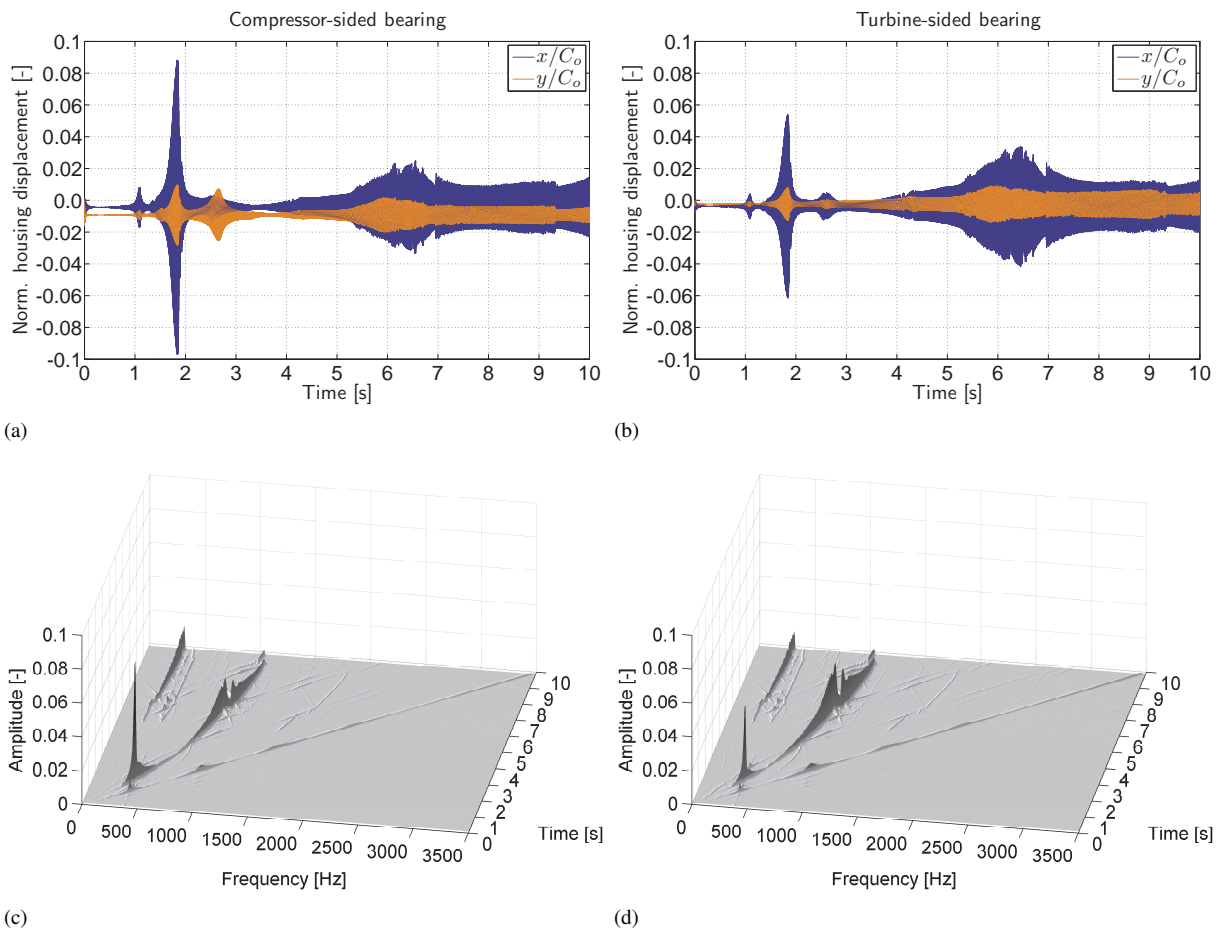


Figure 7: Run-up simulation of complete system (housing subsystem): (a) Normalized housing displacement at compressor-sided bearing. (b) Normalized housing displacement at turbine-sided bearing. (c) Waterfall diagram of displacement in  $x$ -direction from plot (a). (d) Waterfall diagram of displacement in  $x$ -direction from plot (b).

- At the resonance peaks excited by Sub 2, the response frequencies abruptly changes as already noticed for the rotor oscillations, see Figure 6.

In general, the results of the complete system show qualitatively the same behavior as for the decoupled approach and only slightly differ quantitatively. Therefore, the sequential simulation of both subsystems builds a very good approximation and can be applied to evaluate the vibro-acoustical behavior of the turbocharger housing.

For comparison purposes, the displacements are plotted on both measurement points at the housing in Figure 8. Here, the housing amplitudes are also insignificantly decreased in comparison with the decoupled approach.

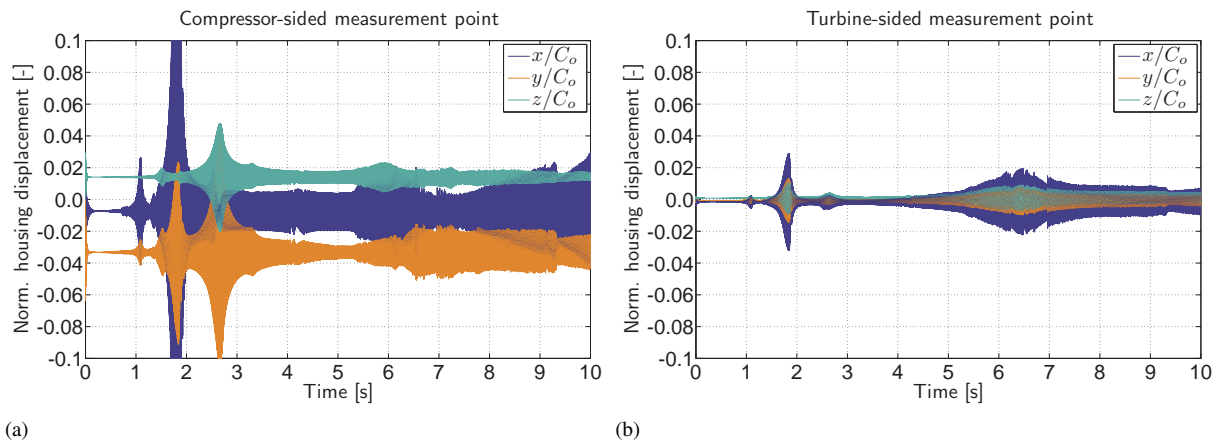


Figure 8: Normalized housing displacements for run-up simulation of complete system: (a) Compressor-sided measurement point. (b) Turbine-sided measurement point.

#### 4 Conclusion

In this paper, the housing structure is additionally considered in the run-up simulation of a turbocharger rotor to investigate the dynamical and the vibro-acoustical behavior. The synchronous and subsynchronous oscillations of the rotor bearing system are transmitted through the oil film forces to excite the eigenfrequencies of the housing subsystem. In the considered passenger-car turbocharger, the Sub 2 excitation is critical due to its higher amplitudes. Furthermore, the response amplitudes of the housing subsystem are magnified by a resonance of an out-of-phase bending mode whose eigenfrequency lies in the speed range of the Sub 2 excitation. Since the Sub 2 frequency slightly increases with higher rotor speeds this resonance leads to a magnification in a relatively wide speed range which is well-known as constant-tone phenomenon. The excitation frequencies of Sub 1 and Sub 3 are too low to excite housing resonances. The synchronous excitation due to unbalance is passed through very quickly. Therefore, the turbocharger design demands to avoid magnification with regard to acoustic problems by shifting the housing's eigenfrequencies out of the Sub 2 excitation frequency range.

Besides the findings described above, two more conclusions can be drawn concerning a simulation of the decoupled subsystems rotor and housing. First, the influence of bearing shell deformation is negligible in the run-up simulation of turbocharger rotors if an instability phenomenon like Total Instability does not occur where extremely high oil film forces are reached. Second, a sequential computation of the two subsystems rotor and housing provides appropriate results. In future studies, a more sophisticated acoustic simulation of the turbocharger housing can follow a run-up simulation of the rotor subsystem assuming rigid bearing shells.

#### References

- Ascher, U. M.; Petzold, L. R.: *Computer methods for ordinary differential equations and differential-algebraic equations*. Society for Industrial and Applied Mathematics, Philadelphia (1998).
- Boyaci, A.: Numerical continuation applied to nonlinear rotor dynamics. *Procedia IUTAM*, 19, (2016), 255 – 265.
- Boyaci, A.; Hetzler, H.; Seemann, W.; Proppe, C.; Wauer, J.: Analytical bifurcation analysis of a rotor supported by floating ring bearing. *Nonlinear Dynamics*, 57, (2009), 497 – 507.

- Boyaci, A.; Lu, D.; Schweizer, B.: Stability and bifurcation phenomena of Laval/Jeffcott rotors in semi-floating ring bearings. *Nonlinear Dynamics*, 79, (2015), 1535 – 1561.
- Boyaci, A.; Schweizer, B.: *Proceedings of the 9th IFToMM International Conference on Rotor Dynamics*, chap. Nonlinear oscillations of high-speed rotor systems in semi-floating ring bearings, pages 845 – 854. Springer (2015).
- Boyaci, A.; Seemann, W.; Proppe, C.: *IUTAM Symposium on Emerging Trends in Rotor Dynamics*, chap. Bifurcation analysis of a turbocharger rotor supported by floating ring bearings, pages 335 – 347. Springer Netherlands (2011).
- Chasalevris, A.: Finite length floating ring bearings: Operational characteristics using analytical methods. *Tribology International*, 94, (2016), 571 – 590.
- Chatzisavvas, I.; Boyaci, A.; Koutsovasilis, P.; B., S.: Influence of hydrodynamic thrust bearings on the nonlinear oscillations of high-speed rotors. *Journal of Sound and Vibration*, 380, (2016), 224 – 241.
- Childs, D.: *Turbomachinery rotordynamics*. Wiley-Intersciences, New York (1993).
- Craig, R. R.; Bampton, M. C.: Coupling of substructures for dynamics analyses. *AIAA Journal*, 6, (1968), 1313 – 1319.
- DuBois, G. B.; Ocvirk, F. W.: Analytical derivation and experimental evaluation of short-bearing approximation for full journal bearing. *NACA Report*, 1157, (1953), 1199 – 1206.
- Gear, C. W.; Leimkuhler, B.; Gupta, G. K.: Automatic integration of euler-lagrange equations with constraints. *Journal of Computational and Applied Mathematics*, 12&13, (1985), 77 – 90.
- Kirk, R. G.; Alsaeed, A. A.; Gunter, E. J.: Stability analysis of a high-speed automotive turbocharger. *Tribology Transactions*, 50, (2007), 427 – 433.
- Köhl, W.; Kreschel, M.; Filsinger, D.: Experimental and numerical investigations on an automotive turbocharger with a transparent bearing section. In: *11th International Conference on Turbochargers and Turbocharging*, pages 349 – 359, Woodhead Publishing, Oxford (2014).
- Koutsovasilis, P.; Driot, N.; Lu, D.; Schweizer, B.: Quantification of sub-synchronous vibrations for turbocharger rotors with full-floating ring bearings. *Archive of Applied Mechanics*, 85, (2015), 481 – 502.
- Nguyen-Schäfer, H.: *Aero and vibroacoustics of automotive turbochargers*. Springer, Berlin (2013).
- Nowald, G.; Boyaci, A.; Schmoll, R.; Koutsouvasilis, P.; Schweizer, B.: Influence of circumferential grooves on the non-linear oscillations of turbocharger rotors in floating ring bearings. In: *The 14th IFToMM World Congress*, Taipei, Taiwan (October 2015).
- Orcutt, F. K.; Ng, C. W.: Steady-state and dynamic properties of the floating-ring journal bearing. *ASME Journal of Lubrication Technology*, 90, (1968), 243 – 253.
- San Andrés, L.; Rivadeneira, J. C.; Chinta, M.; Gjika, K.; LaRue, G.: Nonlinear rotordynamics of automotive turbochargers: predictions and comparisons to test data. *ASME Journal of Engineering for Gas Turbines and Power*, 129, (2007), 488 – 493.
- Schweizer, B.: Total instability of turbocharger rotors - physical explanation of the dynamic failure of rotors with full-floating ring bearings. *Journal of Sound and Vibration*, 328, (2009), 156 – 190.
- Schweizer, B.: Dynamics and stability of automotive turbochargers. *Archive of Applied Mechanics*, 80, (2010), 1017 – 1043.
- Shabana, A.: *Dynamics of multibody systems*. Cambridge University Press, Cambridge (2005).
- Tanaka, M.; Hori, Y.: Stability characteristics of floating bush bearings. *ASME Journal of Lubrication Technology*, 93, (1972), 248 – 259.
- Woschke, E.; Göbel, S.; Nitzschke, S.; Daniel, C.; Strackeljan, J.: *Proceedings of the 9th IFToMM International Conference on Rotor Dynamics*, chap. Influence of bearing geometry of automotive turbochargers on the non-linear vibrations during run-up, pages 835 – 844. Springer (2015).